Targeting Nucleolin Improves Sensitivity to Chemotherapy in Acute Lymphoblastic Leukemia

Yanxin Chen
Fujian Institute of Hematology
Zhengjun Wu
Fujian Institute of Hematology
Lingyan Wang
Fujian Institute of Hematology
Minhui Lin
Fujian Institute of Hematology
Peifang Jiang
Fujian Institute of Hematology
Jingjing Wen
Fujian Institute of Hematology
Jiazheng Li
Fujian Institute of Hematology
Yunda Hong
Fujian Institute of Hematology
Xiaoyun Zheng
Fujian Institute of Hematology
Xiaozhu Yang
Fujian Institute of Hematology
Jing Zheng
Fujian Institute of Hematology
Robert Peter Gale
Imperial College London
Ting Yang
Fujian Institute of Hematology
Jianda Hu (drjiandahu@163.com)
Fujian Institute of Hematology https://orcid.org/0000-0002-9319-7062

Research Article

Keywords: acute lymphoblastic leukemia, nucleolin, resistance, ERK signaling, AS1411

Posted Date: May 20th, 2022

DOI: https://doi.org/10.21203/rs.3.rs-1632324/v1

Abstract

Most acute lymphoblastic leukemia (ALL) patients are treated with chemotherapy as primary care. Although treatment response is usually positive, resistance and relapse often occur through unclear mechanisms. Here, we presented clinical and experimental evidence that overexpression of nucleolin (NCL), a multifunctional nucleolar protein, is linked to drug resistance in ALL. By analyzing our patient specimens and an existing database, a strong correlation between the abundance of nucleolin and disease relapse/poor survival was observed. Altering the NCL expression resulted in changes in drug sensitivity in cell lines. High levels of nucleolin could up-regulate components of the ATP-binding cassette transporters via the activation of the ERK pathway, which resulted in a decrease in drug accumulation inside the cells. NCL protein was mainly distributed in the cytoplasm and membrane in ALL cells compared with cell nuclei of normal cells. Moreover, targeting NCL with AS1411, a nucleolin-binding oligonucleotide aptamer, drastically increased sensitivity to chemotherapeutic drugs in cells/patients derived xenograft mice and extended survival of the diseased mice. Our results indicated that NCL could be a prognostic marker and provided initial preclinical evidence that inhibiting nucleolin expression could enhance drug sensitivity during ALL chemotherapy.

Background

Compared to the favorable survival in pediatric acute lymphoblastic leukemia (ALL)[1], the prognosis of adult ALL remains unsatisfactory[2]. Immunotherapy provides a promising outcome for relapsed/refractory(R/R) ALL[3;4], but it is associated with high relapse frequency and limited long-term survival rate[5]. Chemoresistance is the principal cause of ineffectiveness in treatment. Numerous factors, such as genetic alteration or overexpression of membrane ATP-binding cassette (ABC) transporters, may be responsible for the development of chemo-resistance[6;7].

Human nucleolin (NCL) is a multifaceted protein that localizes in various cellular compartments and can interact with DNA, RNA, and protein[8;9]. NCL plays an important role in ribosome biogenesis, mRNA translation, signal transduction, and cell proliferation[10–12]. Our previous studies have revealed that NCL is upregulated in the drug-resistant myeloid leukemia cell line HL-60[13]. However, the impact of NCL on drug resistance, especially anthracyclines resistance in ALL is unstudied. In the present study, we aimed to test the hypothesis that high expression of NCL contributes to drug resistance in ALL.

We detected the NCL expression in the newly diagnosed and relapsed/refractory ALL patients and identified that NCL was positively correlated with the ALL progression and unfavorable prognosis. In addition, the underly mechanisms of NCL in drug resistance were investigated both *in vitro* and in cell lines/patients derived xenograft model by developing two drug-resistant ALL cell lines and altering NCL expression in ALL cell lines. Our results showed that nucleolin up-regulated components of the ATP-binding cassette transporters via the activation of the ERK pathway, decreased drug sensitivity and promoted ALL progression.

Methods

Primary cells collection

Mononuclear cells were isolated from the bone marrow or peripheral blood of patients with ALL with *de novo* diagnosed (ND) and relapsed/refractory (R/R) status, or bone marrow from complete remission (CR), or peripheral blood from healthy donors in the Department of Hematology, which was approved by the Ethics Committee and the Institutional Review Board of Fujian Medical University Union Hospital (2014058). All patients provided informed consent by the Declaration of Helsinki. ALL was diagnosed based on guidelines of the Chinese Medical Association and National Comprehensive Cancer Network (NCCN)[14]. Subject received ≥ 1 course of chemotherapy under protocol CALLG2008 of the Chinese Acute Lymphoblastic Leukemia Cooperative Group[15]. ND or R/R patient specimens with over 80% leukemia cells after isolation were included in the analysis. Blood and bone marrow samples' mononuclear cells were purified by Ficoll-Paque® (GE Healthcare, Chicago, IL, USA) density-gradient centrifugation and proteins isolated as described [16].

Cell culture

Human T-ALL cell lines Jurkat and Molt-4, B-ALL cell line Nalm-6, BALL-1 and B-lymphoblast cells Hmy2.CIR with short tandem repeat (STR) certification and checking for negative mycoplasma contamination were preserved in the Fujian Institute of Hematology and cultured in RPMI 1640 medium supplemented with 10% fetal bovine serum at 37°C with 5% CO_2. Molt-4 and Nalm-6 cells were exposed to stepwise increasing concentrations of adriamycin to develop resistant cell lines. Single-cell clones were developed by limiting dilution[17]. Adriamycin-resistant Molt-4 and Nalm-6 cell clones were designated Molt-4/ADR(MAR) and Nalm-6/ADR(NAR). Adriamycin (ADR), 1 μg/ml, was used to maintain resistance[16].

Vector construction

Full-length human NCL cDNA (2,174 bp) was synthesized by the polymerase chain reaction (PCR) inserted into a lentiviral-GV320-Cherry expression vector and designated LV-NCL-OE for over-expression of NCL. The empty vector for the negative control was designated LV-NC. A plasmid expressing short hairpin RNA (shRNA) targeting NCL was constructed by inserting double-stranded oligonucleotides into a lentiviral pGCL-tet-puro-EGFP vector and designated LV-shNCL. The plasmid carrying the non-targeting scramble sequence was designated LV-shNT. Lentiviral vectors were produced in HEK293T cells by transient transfection of the relevant plasmids. Primer sequences are displayed in Supplement Table S1.

Developing stable cell lines

Jurkat, Molt-4, and Nalm-6 cells were transfected with lentiviral particles LV-NCL-OE carrying the NCL cDNA or the empty vector LV-NC to produce NCL-overexpressing cells designated over-expression (OE) or negative control (NC). Jurkat, Molt-4, Nalm-6, and Molt-4/ADR cells were transfected with LV-shNCL, or

LV-shNT (as negative control) to produce shRNA-expressing cells designated knockdown (KD) or Scramble (Scr). Transfected cells were selected in the presence of puromycin, 0.3 μg/ml, and expression of shRNA induced by adding 2 μg/ml of doxycycline for 24 h followed by maintenance in a complete medium containing puromycin, 0.2 μg/ml, and doxycycline, 2 μg/ml.

The half-maximal inhibitory concentration (IC_{50}) assay

4×10^4 cells were cultured in the presence of adriamycin, dexamethasone, vincristine, L-asparaginase, and methotrexate at various concentrations for 48 h. Cells were added to 10 μl of a solution containing 3-(4,5-dimethylthiazol-2-yl)-2,5 diphenyltetrazolium bromide (MTT, Sigma, MO, USA) and incubated for 4 h. 100 μl dimethyl sulfoxide (DMSO, Sigma) was added to dissolve formazan crystalline, and absorbance was measured using Elx808 Absorbance Microplate Spectrophotometer (BioTek, Winooski, VT, USA) at reference wavelengths of 490 and 630 nm[22] and optical density (OD) values determined. Inhibitory rates were calculated according to the following formulae: (1– OD drug-treated cells/ OD untreated cells) ×100%. Change in drug sensitivity was expressed by taking the ratio of IC50 values of the *NCL* over-expressing or knock-down cells *versus* control.

Intra-cellular adriamycin accumulation assay

Intra-cellular adriamycin accumulation was determined using a BD FACSCalibur (Becton Dickinson, Franklin Lakes, NJ, USA). Cells were cultured at a density of 5.0×10^5 cells/ml in the presence of 0, 0.5, or 1 μg/ml adriamycin for 12 h, collected and washed twice for multi-parameter flow cytometric (MPFC) analyses. DAPI buffer was used to stain DNA. Adriamycin mean fluorescence intensity (MFI) was analyzed using the FlowJo software 7.6.1. (Tomy Digital Biology, Tokyo, Japan).

Rhodamine-123 efflux assay

A rhodamine-123 efflux assay was used to study the function of ABC transporters. Cells were incubated at 5×10^5 cells/ml with 1 μmol/L rhodamine-123 (Sigma-Aldrich, St. Louis, MO, USA) in RPMI-1640 medium at 37°C for 30 min, washed and incubated in the rhodamine-123-free medium at 37°C for 60 min, and analyzed in MPFC. Unexposed cells were negative controls. Results were analyzed using the FlowJo software.

Quantitative Real-time PCR (qRT-PCR)

Total cell RNA was isolated using TRIzol reagent (Invitrogen, Carlsbad, CA, USA) according to the manufacturer's protocol. cDNA was synthesized from 1μg RNA using the GoScript™ reverse transcription system (Promega, Madison, WI, USA). cDNA was mixed with 2 × SYBR Green PCR Master Mix (Applied Biosystems, Thousand Oaks, CA, USA) with gene-specific primers. qRT-PCR was run using AB 7500 Real-Time PCR system (Applied Biosystems). Samples were run in triplicate and normalized using 18S rRNA. Primer specificity was verified by melting curve analyses. Relative gene expression was determined

using the comparative threshold cycle (Ct) and $2^{-\Delta\Delta Ct}$ method. Primer sequences are displayed in Supplementary Table S1.

Western blotting

Western blotting was performed as described[21]. β-actin, GADPH, NCL, and BCRP antibodies were from Santa Cruz Technology (Dallas, TX, USA), α-Tublin, Histone H3, phospho-ERK1/2, ERK1/2, phospho-Raf, Raf, phospho-MEK1, and MEK1 from Cell Signaling Technology (Danvers, MA, USA), and Ras, P-gp, MRP1, and LRP from Abcam Inc. (Cambridge, UK). Anti-mouse and anti-rabbit secondary antibodies were used following the manufacturer's instructions (Abcam Inc.). Immune reactivity was detected by chemiluminescence reaction using an enhanced chemiluminescence (ECL) kit (Pierce, Rockford, IL, USA).

Pathway suppression assay

Cells were cultured at a density of 1×10^6 cells/ml in media containing 10 nM SCH772984 ERK1/2 inhibitor, 10nM GSK1120212 MEK1/2 inhibitor, 100nM PLX-4720 B-Raf^{V600E} inhibitor (Selleck Chemicals, TX, USA) or mock medium control in triple 6-well plates. 1 µg/ml ADR was added to one plate and cells were cultured for 12 h and analyzed for intra-cellular adriamycin accumulation (described above). Cells of the other two plates were cultured for 48 h and analyzed for RNA and protein concentrations by qRT-PCR and western blotting after inhibiting the ERK pathway.

Immune precipitation analyses

Protein co-immune precipitation analyses to detect the interactions between nucleolin and other proteins were done by Crosslink Magnetic IP/Co- IP Kit (Pierce, Rockford, IL, USA) according to manufacturer's protocol. Briefly, monoclonal antibodies (5 µg) were coupled to pre-washed protein A/G magnetic beads for 15 minutes and cross-linked with disuccinimidyl suberate (DSS) for 30 minutes. Antibody-crosslinked beads (25 µl) were incubated with 500 µl cell lysate from 10 million cells overnight at 4°C on a rotator. The beads were washed, and the bound proteins were eluted from the beads in elution buffer for 5 minutes at room temperature and then neutralized with buffer. Eluates were used for western blot analyses.

Immune fluorescence staining

2×10^5 Jurkat, Molt-4, Nalm-6, and Hmy2.CIR cells were fixed in 4% paraformaldehyde for 15 min at room temperature and permeabilized with 0.2% Triton X-100 in PBS for 10 min. Non-specific binding of the antibody was blocked with 1% bovine serum albumin and 5% goat serum in PBS for 1 h at room temperature. Dishes were incubated overnight at 4°C with primary anti-*NCL* antibody (1:100 dilution in blocking buffer), washed in PBS, and incubated with secondary PE-conjugated goat anti-mouse IgG (diluted 1:500 in blocking buffer) for 1 h at room temperature. DAPI buffer (10 µg/mL) was used to stain DNA. Cells were washed thrice in PBS and studied using a fluorescence microscope. Images were overlaid.

Plasm& membrane (PM) and Nuclear (N) protein extraction

Intracellular expression of NCL protein was done by Nuclear and Cytoplasmic Protein Extraction Kit (Beyotime, Shanghai, CN) according to manufacturer's protocol. Briefly, PM and N proteins were extracted by cytoplasm lysis buffer and nuclear lysis buffer respectively with 5×10^6 Jurkat, Molt-4, Nalm-6, BALL-1, Hmy2.CIR cells and PBMC from healthy donors or patients with ALL. The extractions were used for western blot analyses with 20μg/test. α-tubulin protein was used as loading control of cytoplasm protein(diluted 1:400 in blocking buffer). Histone H3 protein was used as loading control of nuclear protein (diluted 1:1000 in blocking buffer).

Membrane NCL staining assay by flow cytometry

1×10^6 Jurkat and primary ALL cells from relapsed-refractory ALL patients were incubated with 5μl anti-NCL-FITC (Biolegend, CA, US) or isotype control at 4°C for 15min. Cells were washed and detected using a BD FACSCalibur (Becton Dickinson, Franklin Lakes, NJ, USA), and analyzed using the FlowJo software 7.6.1. (Tomy Digital Biology, Tokyo, Japan).

Mouse xenografts

BALB/C nude mice (SLAC Laboratory Animal, Shanghai, China) were injected subcutaneously with 8×10^5 Nalm-6 or Nalm-6/ADR cells. Treatments were started after tumor volume reached about 100-300 mm^3. Tumor volumes= shortest $diameter^2$ × longest diameter/2. Nalm-6 nude mice (n=5) were received vehicle, adriamycin(1.5 mg/kg), aptamer control sequence (CCT-rich sequence, CRO, Sangon,15 μg *per* mouse), aptamer AS1411(15 μg *per* mouse) only, adriamycin with CRO or AS1411(Applied Adriamycin followed by AS1411 or CRO), respectively. For Nalm-6/ADR model, mice were divided into 7 cohorts each of 6 mice. Mice received AS1411, 75 μg *per* mouse and CRO, 75 μg *per* mouse. Adriamycin was injected intravenously *via* the tail vein once a day for 3 days. Aptamers were given by subcutaneous injection adjacent to the tumor daily for 7 days. Tumor suppression rate (%) = (1- mean tumor weight in cohort/mean tumor weight in controls) ×100%.

NCG mice (Nanjing Biomedical Research Institute, Nanjing, China) were injected intravenously with 1×10^4 Nalm-6 cells stably expressing firefly luciferase. One week later mice were injected with vehicle, adriamycin (1.5 mg/kg intravenously daily for 3 d), AS1411 (15 μg *per* mouse daily subcutaneously proximal to the tumor for 7 d) or the sequential combination of adriamycin and AS1411. Leukaemia development was monitored using the IVIS imaging system (PerkinElmer, Hopkinton, MA, USA). Human CD45+ (hCD45-positive) cells were detected in mouse bone marrow by MPFC as described. Moribund mice were euthanized and hCD45-positive leukaemia cells in spleen and bone marrow were analyzed by MPFC.

1×10^6 patients-derived xenograft (PDX) expanded B-ALL cells were injected *via* the tail vein into NOD-*scid-IL2Rg-/-*(NSI) mice ages 8–10 weeks immediately after exposure to 1 Gy total body radiation. Two weeks later mice received adriamycin, 1.5 mg/kg intravenously daily for 3 d, AS1411 or CRO, 15 μg *per*

mouse daily subcutaneously proximal to the tumor for 7 d or adriamycin, 1.5 mg/kg intravenously, daily for 3 d followed by AS1411, 15 μg *per* mouse daily subcutaneously proximal to the tumor daily for 7 d. Blood cells were sampled weekly to assess leukaemia.

All experiments were approved by the Ethics Committee of Institutional Animal Care and Use. BALB/C nude mice and NCG mice experiments complied with guidelines of Fujian Medical University. NSI mouse experiments complied with guidelines of the Laboratory Animal Center of the Guangzhou Institutes of Biomedicine and Health (GIBH).

Statistical analyses

Overall survival (OS) was defined as the interval from diagnosis to death or censored at transplant or last follow-up. Relapse-free survival (RFS) was defined as the interval from complete remission to relapse or death from any cause or transplant. Survival analysis of the patients was constructed using the R software, with the survival and survminer packages. Kaplan-Meier plots were created to illuminate the correlations between the genetic risk scores and the survival index of patients, including OS and RFS12. Univariate and multivariate COX regression analyses were used to test whether the genetic risk score model is an independent prognostic risk factor relative to the clinical characteristics of the total set. Statistical significance was tested using log-rank tests. The prognostic risk factors were analyzed using Cox Regression with the survival R packages. A p-value < 0.05 was considered to be statistically significantly different.

Experiments were done in triplicate. Concentrations were expressed as mean ± SEM (standard error mean) or median (interquartile range [IQR]). Students *t*-test, one-way analysis of variance (ANOVA), Kruskal–Wallis or chi-square tests were used as appropriate. Data were analyzed using SPSS statistics software 23.0 (IBM, Chicago, IL, USA) or GraphPad Prism Software 6.0 (GraphPad, San Diego, CA, USA).

Results

High expression of NCL is associated with inferior disease status and poor survival in ALL

To obtain NCL expression information and treatment response, we analyzed 223 specimens from ALL patients with ND, CR, and R/R disease (Supplementary Fig. S1). mRNA level of NCL in ND ALL was quantitatively higher than in CR status, and R/R ALL had the highest level (P<0.05; Fig. 1A), indicating a remarkable increasing expression of NCL mRNA at refractory/relapsed disease. Following a similar trend, the highest level of NCL protein was observed in the R/R patients. The healthy donors showed no expression of NCL protein (Fig. 1B, C). For external validation, we downloaded the mRNA expression dataset (GSE163634) from the GEO database (https://www.ncbi.nlm.nih.gov/geo/). The data from GSE163634 were based on the GPL16791 platforms and included data of 55 samples at newly diagnosed(n=23) and relapsed (n=32) from 28 patients with ALL. NCL mRNA levels were significantly increased in the relapsed group (P=0.0303) when compared to the de novo group. Longitudinal specimens' analysis indicated that NCL mRNA levels tended to elevate in the patients (n=22) at relapse

when compared to their corresponding de novo samples(P=0.0552). Thus, both RNA and protein measurements supported that elevated NCL expression is linked to ALL disease status.

To evaluate the prognostic value of NCL expression in ALL, the median value of relative NCL mRNA expression was defined as the cutoff value for dividing ND ALL patients into high- and low- expression groups (Supplementary Table. S2). The NCL-high group has significantly poorer 2- year OS (28.23% vs 50.54%, *P*=0.033) and 2-year RFS (5.02% vs 18.67%, *P*=0.027; Fig 1F, G) than those with low NCL mRNA expression. For external validation, we downloaded the mRNA expression dataset of 362 pediatric B-cell ALL patients and their corresponding clinical information from the TARGET database (https://ocg.cancer.gov/programs/target)(Supplementary Table.S3.). The data of 362 cases were based on the GPL570 platform. NCL expression was positively correlated with a high WBC count at diagnosis (P=0.0077). Kaplan-Meier curves indicated that patients with high NCL expression had a remarkably shorter 5-year OS (38.72% vs 83.25%, P=0.005) than the patients with low NCL expression (Fig. 1H). Moreover, univariate analysis of the dataset from TARGET showed that high NCL expression(P=0.001) and positive of minimal residual disease (MRD) at D29 (P=0.092) after initial treatment were significant predictors of inferior OS (Fig. 1I). In multivariate analysis, high NCL expression remained an independent unfavorable predictor of OS (P<0.0001, Fig. 1J). Together, NCL was correlated with disease progression and indicated inferior survival in ALL.

NCL levels were inversely correlated with the sensitivity of chemotherapeutics in multiple ALL cell lines

The parental Molt-4 and Nalm-6 cells had significantly lower levels of NCL than the MAR and NAR cells, respectively, indicating a relationship between NCL and drug resistance in ALL (Supplementary Fig. S3).

Next, we tested whether ectopic overexpression of NCL could alter the ADR sensitivity of leukemia cell lines. Both qPCR and immunoblotting revealed that the OE cells of all three ALL cell lines that harbored the NCL constructs had significant increases in IC50 relative to three of the corresponding NC lines. We then tested whether knocking down NCL expression may affect the sensitivity of ALL cells to ADR. NCL knockdown in Jurkat, Molt-4 and Nalm-6 cell lines led to significantly increased sensitivity to ADR. We also tested whether NCL knockdown would re-sensitize the drug-resistant MAR cells. The resistant MAR cells became almost as sensitive to ADR as the sensitive parental Molt-4 cells when NCL was downregulated (Supplementary Fig. S3).

Besides, we identified whether NCL could affect the sensitivity of other key agents in the standard chemotherapy regiment of ALL, including VDS, MTX, DEX, and L-ASP in NCL overexpression or suppression of Jurkat and Molt-4 and Nalm-6cells . As expected, overexpression of NCL decreased the drug sensitivity while knockdown of NCL increased the drug sensitivity of the above chemo-agents, suggesting that NCL may affect the multidrug sensitivity of ALL cells (Supplementary Fig. S4).

Collectively, these results established that the NCL level, per se, affected the sensitivity of ALL cells to the multiple chemo-agents, and are consistent with our clinical observation that relapsed/refractory ALL patients had a higher NCL level than CR patients.

NCL facilitated drug efflux from ALL cells by regulating ABC transporters

In addition to assessing the drug sensitivity of the aforementioned NCL OE and KD cell lines, we also analyzed ADR accumulation inside cells by taking advantage of the fact that the ADR molecule has a natural fluorophore moiety, which greatly facilitates flow cytometry[16]. For all three of the OE lines (Jurkat and Molt-4 and Nalm-6), flow cytometry revealed that the intracellular ADR MFI were significantly reduced when compared to corresponding NC cells. In direct contrast, we observed significant increases in ADR MFI when compared with the various NCL KD cells against the corresponding Scr cells (Fig. 2A and 2B).

To further confirm the effect of NCL on drug efflux, we conducted classic rhodamine-123 tracer dye experiments with the Jurkat and Nalm-6 KD cells[18], and again observed that NCL knockdown resulted in increased cellular accumulation of the tracer dye, and *vice versa* upon the OE cells and their controls (Fig. 2C and 2D). These identical NCL-related trends for the efflux of two compounds strongly suggested the involvement of NCL in the function of drug efflux pump ABC transporters.

We investigated whether the four well-known ABC transporters, MDR1, BCRP, LRP, and MRP1[19;20], might have been involved in the observed drug accumulation changes. The Molt-4, Jurkat, and Nalm-6 OE cells consistently showed significant increases in *BCRP, LRP*, and *MRP1* mRNA expression compared to the corresponding NC cells. Increases in protein levels were also detected in Molt-4 and Jurkat OE cells. However, MDR1 RNA and protein were not detected in Molt-4 or Jurkat cells, even when NCL was overexpressed (Fig. 3A, 3B, and 3C).

Furthermore, we detected significant decreases in the expression of *BCRP*, *LRP*, and *MRP1* transcripts in the Jurkat and Nalm-6 KD cells compared to their Scr shRNA control cells. The level of MDR1 protein (P-glycoprotein; P-gp) was high in MAR cells but drastically reduced after NCL KD (Fig. 3D). Wherein we re-transfected Jurkat KD cells and Nalm-6 KD cell with an expression vector of a codon-alternative variant of NCL designed to be resistant to silencing by the NCL-shRNA. We observed that this rescue recovered NCL expression at both the mRNA and protein levels and further significantly recovered the expression of BCRP (Supplementary Fig. S5). Thus, NCL contributes to the drug efflux capacity of ALL cells by positively regulating the expression of genes encoding ABC transporters.

NCL regulated the abundance of ABC transporters via the ERK pathway

Given the frequent involvement of ERK signaling in drug resistance mechanisms[21], we examined the extracellular signal-related kinase ERK pathway. Compared to the control, the NCL-OE Jurkat and Molt-4 cells showed elevated phosphorylation of Raf, MEK1/2, and ERK (Fig. 4A and Supplementary Fig. S6). Consistently, the NCL-KD Jurkat cells exhibited less phosphorylation (Fig. 4A). We also examined the interaction between NCL and ERK by immunoprecipitation. ERK immunoprecipitated with NCL, and vice versa (Fig. 4B and 4C). These data suggested that NCL binds, directly or indirectly, to ERK (and perhaps Ras as well, Fig. 4C) and stimulates ERK signaling.

We then tested whether ERK signaling was linked to ABC transporters and intracellular drug accumulation by treating the Jurkat OE cells with SCH772984 (an ERK inhibitor), GSK1120212 (a MEK inhibitor), or PLX-4720 (a Raf inhibitor). All three inhibitors caused a decrease in MRP1 and BCRP levels (Fig. 4D, protein; Fig. 4G and 4H, RNA), as well as an increase in ADR accumulation (Fig. 4E). Interestingly, none of these inhibitors affected NCL expression (Fig. 4D and 4F). These data suggested that NCL could regulate the ERK signals for ABC transporter-mediated drug resistance.

Targeting NCL increased drug sensitivity in ALL cells and NCL inhibitor-based combination therapies sensitized ALL cells to ADR

We analyzed the intracellular location of NCL protein in the ALL cell lines and blast cells using immunofluorescence staining, flow cytometry, and western blotting. The results indicated that nucleolin was presented mainly in the cytoplasm and membrane of ALL cells, especially in the membrane. Whereas in normal cells nucleolin was concentrated in nucleus. The concentrated distribution of NCL in the membrane of ALL cells suggested that NCL protein could be a potential biomarker target with well specificity and convenience. (Supplementary Fig. S7)

Further, we tested AS1411, a G-rich oligonucleotide aptamer that binds membrane NCL with high specificity[22;23] and acts as an inhibitor that could be used alone or in combination with an existing drug to inhibit the growth of ALL cells.

Initially, we detected whether treatment with AS1411 affected the KD cells, which were little or no expressed NCL protein in the cell membrane. The KD cells of Jurkat, Molt-4 and Nalm-6 were treated with AS1411(10 μmol/L) or CRO (10 μmol/L), both AS1411 and CRO had no effect on the cellular proliferation, indicating the specificity of targeting NCL using an aptamer (Supplementary Fig. S8). Next, we treated Jurkat cells with AS1411(10 μmol/L) or a negative control CRO with or without ADR. AS1411 did not affect the levels of *NCL* protein in Jurkat cells, but it did significantly sensitize the cytotoxic effects of ADR. Furthermore, flow cytometry revealed that AS1411-treated Jurkat had significantly higher ADR MFIs compared to CRO-treated cells, and the AS1411-treated cells had significantly decreased levels of BCRP protein(Fig. 5A-C).

Moreover, we tested whether inhibition of targeting NCL contributed to improved ADR treatment efficacy. Nalm-6 and NAR cells were treated with AS1411 or CRO with or without ADR. AS1411 inhibited cellular proliferation in Nalm-6 and NAR cells, while the combination with ADR or increased dose (50μmol/L) of AS1411 enhanced the inhibitory effect of AS1411 on NAR cells (Fig. 5 D, F). The ADR IC_{50} values for NAR were decreased with increasing doses of AS1411(Fig. 5 E, G). Flow cytometry revealed that NAR cells treated with increased doses of AS1411 had significantly higher ADR MFIs. (Fig. 5 H, I, J)

These results collectively supported that the inhibition of NCL sensitized resistant NAR to ADR and reversed resistance in ALL cells.

NCL inhibitor-based combination therapies sensitized xenograft mice to ADR

Extending these promising findings *in vitro*, we determined whether inhibition of targeting NCL sensitized ADR treatment for ALL cell-derived xenograft mouse models *in vivo*.

Nalm-6 BALB/C-nude mice with comparable tumor sizes were respectively treated with vehicle, CRO, AS1411, ADR alone, or combination therapy comprising ADR with AS1411 or CRO. Fifteen days after the first dose of treatment, growth of tumor in either ADR- or AS1411-treated group was inhibited significantly by 45.7% (P=0.002) or 37.1% (P=0.008), respectively, compared to the vehicle or control CRO-treated group. Tumor volume in mice with the combination treatment of AS1411 and ADR declined the most dramatically by approximately 79.5% compared to either vehicle (P<0.0001) or ADR alone(P=0.019; Fig. 6 A-D). Similar results were also obtained by tumor weight comparison between each group, which suggested a significantly good efficacy. These data indicated that AS1411 could enhance the ADR antitumor activity in ALL xenografts.

Clinically, the treatment of refractory/relapsed ALL patients is more challenging. Thus, we further tested the efficacy of the combination therapy of AS1411 and ADR in the drug-resistant ALL mouse model established by subcutaneously injecting NAR cells into BALB/C-nude mice. Similar to what we observed in the *in vitro* experiments, tumor volumes in the ADR-treated group were not suppressed significantly (P>0.05; Fig. 6F, G) compared to that of the vehicle-treated group. As shown in Fig. 6G-J, at day 24, the growth of tumors in the high dose (HD) AS1411 or ADR+AS1411 group was inhibited significantly by 60.6% (P=0.007) or 57.6% (P=0.005), respectively, compared to the HD CRO or vehicle group. The maximum tumor suppression rate (78.8%) was achieved by the combination of HD AS1411 and ADR, being more significant than either the vehicle-treated group (P<0.0001) or the ADR-treated group (P=0.042).

We established an orthotopic xenograft model, luciferase-expressing Nalm-6 cells grafted into NCG mice, to further examine the ability of AS1411 to sensitize ADR treatment. As shown in Fig. 6 K-M, AS1411 and ADR monotherapy, as well as the combination treatment, significantly reduced the leukemia burden compared to vehicle treatment (P<0.001), based on the *in vivo* leukemia bioluminescence. Interestingly, ADR combined with AS1411 significantly decreased the counts of human CD45+ cells in mouse bone marrow compared to ADR-treated mice.

Following the same experimental procedure, survival analysis of Luc^{+}Nalm-6 NCG mice that underwent different treatments was conducted. Both AS1411 and ADR monotherapy improved median survival from 27 days in vehicle-treated mice to 31 days (P = 0.042) and 35 days (P = 0.002), respectively (Fig. 6N), whereas mice treated with the dual agents had most significantly extended the median survival of 41 days (P<0.0001, Fig. 6N).

To further identify the effect of AS1411 or sensitize ADR treatment on ALL blast cells *in vivo*, we established PDX models from two relapsed ALL patients (details in Supplementary Table. S4). AS1411 and ADR monotherapy, as well as the combination treatment, could significantly reduce counts of human CD45+ cells in mice peripheral blood compared to CRO-treated mice and vehicle-treated mice (Fig. 7A, B).

FACS revealed more than 90% hCD45+ cells in the bone marrow and spleen in the mice with morbidity (Fig. 7C). The median survival in vehicle-treated mice and ADR monotherapy mice was 24 and 26.5 days respectively. Whereas mice treated with the AS1411 with ADM agents had most significantly extended the median survival of 34 days (P = 0.0047) in the patient1. As to the patient 2, ADR monotherapy improved median survival from 11 days in vehicle-treated mice to 18 days (P = 0.0016) (Fig. 7D). Whereas mice treated with the AS1411 combined ADM agents had extended most significantly median survival of 28 days (P = 0.0016, compared with vehicle-treated mice; P = 0.0019, compared with ADR monotherapy mice.) (Fig. 7E).

Results from two mouse leukemia models clearly indicated that inhibiting NCL with AS1411 resulted in reduced leukemia progression and that a combination therapy comprising AS1411 and ADR offered superior anti-leukemia performance compared to either of these agents as monotherapies.

These results suggested that the NCL-targeting aptamer AS1411 has therapeutic potential in enhancing chemotherapy efficacy, particularly in resistant ALL.

Discussion

Drug resistance of leukemia cells has become a critical hindrance in leukemia treatment, which negatively affects outcomes. Although our understanding of the mechanisms of drug resistance has increased[24–27], the efficacy of reversing drug resistance is limited. Finding novel candidate targets for resolving drug resistance would improve treatment outcomes. Acquisition of multidrug resistance is principally responsible for treatment failure in ALL[28]. Recently, NCL was reported to be related to poor overall survival in solid tumor[29–31] and hematological malignancies DLBCL[23] and AML, particularly in elderly patients[32]. Our group previously demonstrated that NCL is highly expressed in patients with relapsed/refractory acute leukemia as well as in resistant leukemia cell lines[13]; our findings suggested that NCL expression has a prognostic value in predicting treatment outcomes of acute leukemia patients.

In the present study, we focused on the role of NCL in ALL. We found that the NCL level increased in refractory/relapsed ALL patients, suggesting that NCL is a disease status indicator. We also found that NCL-positive patients had inferior OS rates compared to negative patients, suggesting that NCL is a prognostic marker. Experimental results showed the change in drug sensitivity of ALL upon altering the NCL expression. Knockdown increased sensitivity, while overexpression decreased sensitivity. Thus, NCL is involved in the chemotherapy response.

NCL promoted drug resistance by activating the ERK pathway and upregulating the ABC transporter expression. Amplification or overexpression of ABC transporters, such as MDR1, BCRP, MRP1, and LRP, is considered the major mechanism for multiple drug resistance (MDR)[33]. The present study indicates that the levels of MRP1, BCRP, and LRP are positively related to the NCL level. Further, it clarifies the role NCL plays in regulating the expression of ABC transporter proteins by means of an "RNAi rescue experiment," wherein we re-transfected Jurkat KD cells and Nalm-6 KD cell with an expression vector of a codon-

alternative variant of NCL designed to be resistant to silencing by the NCL-shRNA. We observed that this rescue recovered NCL expression at both the mRNA and protein levels and further significantly recovered the expression of BCRP (Supplementary Fig. S5). Nonetheless, our results supported that NCL modulates drug efflux by regulating the expression of ABC transporters in ALL.

The Ras/Raf/MEK/ERK signaling cascade is often hyperactivated in cancer cells, affecting drug resistance[34]. Erk signaling mutation is frequently observed in ALL. NCL stabilizes K-Ras and activates the Ras/MAPK pathway[35]. We proposed the activation of ERK signaling by NCL regulating the expression of ABC transporters. Expression of ABCB1 (*MDR1*) and ABCG2 (*BCRP*) genes is regulated by MAPK/ERK in human ALL cell lines[36]. In the present study, an ERK inhibitor reversed the NCL-mediated reduction of intracellular concentration of ADR and prevented the NCL-mediated increase of BCRP and MRP1. The inhibitor did not affect NCL expression, suggesting that ERK works downstream of NCL. NCL co-localizes with Ras at the intern of the cell plasma membrane and can interact with the Ras protein and ErbB receptors[37]. Our results revealed that NCL interacts with Ras and ERK, acts on the Ras/Raf/MEK/ERK cascade, and regulates the downstream transcription. These results are consistent with findings that NCL promotes drug resistance by activating ERK signaling and upregulating the BCRP and MRP1 genes.

AS1411 is an oligonucleotide aptamer that binds NCL at the cell surface and the complex is internalized[38]. Combining AS1411 with ADR reduces DLBCL cell survival[23]. Our study showed that inhibition of NCL by AS1411 increased ADR accumulation and drug sensitivity in ALL cells, and reduced tumor burden and improved survival in mouse xenografts. Targeting NCL by aptamer AS1411 reverses drug resistance in ALL.

Conclusions

Taken together, we showed that NCL functions as a tumor promoter to propel drug resistance in ALL. With NCL playing a critical role in drug resistance, our study provides a compelling reason to target NCL for treating ALL. Moreover, our findings suggest that therapies employing agents to target NCL offer substantial therapeutic improvements over conventional chemotherapy for ALL.

Declarations

Ethics approval and consent to participate

All the experiments were approved by the review board of the approved by the Ethics Committee and the Institutional Review Board of Fujian Medical University Union Hospital. All animal experiments were approved by the Ethics Committee of Institutional Animal Care and Use. BALB/C nude mice and NCG mice experiments were carried out following the guidelines of the animal facility at Fujian Medical University. NSI mice experiment were carried out following the guidelines of the animal facility in the Laboratory Animal Center of the Guangzhou Institutes of Biomedicine and Health (GIBH). All patients gave written informed consent for the use of their clinical specimens for medical research.

Consent for publication

Written informed consent for publication was obtained from the patients. All authors have agreed to publish this manuscript.

Availability of data and material

All data and material have been provided in the manuscript and supplement materials.

Conflict of interests

Conflict-of-interest disclosure: RPG is a consultant to BeiGene Ltd., Fusion Pharma LLC, LaJolla NanoMedical Inc., Mingsight Parmaceuticals Inc. and CStone Pharmaceuticals; advisor to Antegene Biotech LLC, Medical Director, FFF Enterprises Inc.; partner, AZAC Inc.; Board of Directors, Russian Foundation for Cancer Research Support; and Scientific Advisory Board: StemRad Ltd.

Funding

This work was supported by Supported by National Natural Science Foundation of China (81870135, 81470326, U2005204,82000142), Natural Science Foundation of Fujian Province(2020J05049), National Key Clinical Specialty Discipline Construction Program (2021-76), Fujian Provincial Clinical Research Center for Hematological Malignancies (2020Y2006).

Authors' contributions

Contributions: JDH. and YXC conceived and designed the experiment; YXC, LYW., JJW. and YDH Did the *in vitro* experiments and data analyses. ZJW performed the animal experiments and data analyses. LYW, JZL and PFJ constructed the adriamycin resistant cells. MHL and YXC collected samples and quantified NCL expression. YXC analyzed the clinical data. XYZ, YZY, JZ and TY provided and analyzed clinical samples and data. YXC, ZJW and RPG prepared the typescript. All authours approved the final typescript and agreed to submit for publication.

Acknowledgements

We thank subjects and normals for donating. Profs. Ren-Jiang Lin (City of Hope, California), and Hsin-An Hou (Taiwan University Hospital) provided scientific discussion and reviewed the typescript. RPG acknowledges support from the National Institute of Health Research (NIHR) Biomedical Research Centre funding scheme.

References

1. Girardi T, Vicente C, Cools J, De Keersmaecker K. The genetics and molecular biology of T-ALL. Blood. 2017;129(9):1113–23.

2. Pui CH, Nichols KE, Yang JJ. Somatic and germline genomics in paediatric acute lymphoblastic leukaemia. Nat Rev Clin Oncol. 2019;16(4):227–40.
3. Ghorashian S, Kramer AM, Onuoha S, et al. Enhanced CAR T cell expansion and prolonged persistence in pediatric patients with ALL treated with a low-affinity CD19 CAR. Nat Med. 2019;25(9):1408–14.
4. Kantarjian H, Stein A, Gokbuget N, et al. Blinatumomab versus Chemotherapy for Advanced Acute Lymphoblastic Leukemia. N Engl J Med. 2017;376(9):836–47.
5. Shah NN, Fry TJ. Mechanisms of resistance to CAR T cell therapy. Nat Rev Clin Oncol. 2019;16(6):372–85.
6. Belver L, Ferrando A. The genetics and mechanisms of T cell acute lymphoblastic leukaemia. Nat Rev Cancer. 2016;16(8):494–507.
7. Steinbach D, Legrand O. ABC transporters and drug resistance in leukemia: was P-gp nothing but the first head of the Hydra? Leukemia. 2007;21(6):1172–6.
8. Bian WX, Xie Y, Wang XN, et al. Binding of cellular nucleolin with the viral core RNA G-quadruplex structure suppresses HCV replication. Nucleic Acids Res. 2019;47(1):56–68.
9. Abdelmohsen K, Gorospe M. RNA-binding protein nucleolin in disease. RNA Biol. 2012;9(6):799–808.
10. Brazda V, Haronikova L, Liao JC, Fojta M. DNA and RNA quadruplex-binding proteins. Int J Mol Sci. 2014;15(10):17493–517.
11. Goldson TM, Turner KL, Huang Y, et al. Nucleolin mediates the binding of cancer cells to L-selectin under conditions of lymphodynamic shear stress. Am J Physiol Cell Physiol. 2020;318(1):C83–93.
12. Mariero LH, Torp MK, Heiestad CM, et al. Inhibiting nucleolin reduces inflammation induced by mitochondrial DNA in cardiomyocytes exposed to hypoxia and reoxygenation. Br J Pharmacol. 2019;176(22):4360–72.
13. Hu J, Lin M, Liu T, Li J, Chen B, Chen Y. DIGE-based proteomic analysis identifies nucleophosmin/B23 and nucleolin C23 as over-expressed proteins in relapsed/refractory acute leukemia. Leuk Res. 2011;35(8):1087–92.
14. Brown PA, Wieduwilt M, Logan A, et al. Guidelines Insights: Acute Lymphoblastic Leukemia, Version 1.2019. J Natl Compr Canc Netw. 2019;17(5):414–23.
15. Chinese Society of Hematology CMA, Society of Hematological Malignancies Chinese Anti-Cancer. A. [A Chinese expert panel consensus on diagnosis and treatment of adult acute lymphoblastic leukemia]. Zhonghua Xue Ye Xue Za Zhi. 2012;33(9):789–92.
16. Wang L, Chen B, Lin M, et al. Decreased expression of nucleophosmin/B23 increases drug sensitivity of adriamycin-resistant Molt-4 leukemia cells through mdr-1 regulation and Akt/mTOR signaling. Immunobiology. 2015;220(3):331–40.
17. Linette G, Becker-Hapak M, Skidmore Z, et al. Immunological ignorance is an enabling feature of the oligo-clonal T cell response to melanoma neoantigens. Proc Natl Acad Sci United States Am. 2019;116(47):23662–70.

18. Ju HQ, Zhan G, Huang A, et al. ITD mutation in FLT3 tyrosine kinase promotes Warburg effect and renders therapeutic sensitivity to glycolytic inhibition. Leukemia. 2017;31(10):2143–50.
19. Kourti M, Vavatsi N, Gombakis N, et al. Expression of multidrug resistance 1 (MDR1), multidrug resistance-related protein 1 (MRP1), lung resistance protein (LRP), and breast cancer resistance protein (BCRP) genes and clinical outcome in childhood acute lymphoblastic leukemia. Int J Hematol. 2007;86(2):166–73.
20. Perez DR, Sklar LA, Chigaev A, Matlawska-Wasowska K. Drug repurposing for targeting cyclic nucleotide transporters in acute leukemias - A missed opportunity. Semin Cancer Biol. 2020.
21. Yang T, Xu F, Sheng Y, Zhang W, Chen Y. A targeted proteomics approach to the quantitative analysis of ERK/Bcl-2-mediated anti-apoptosis and multi-drug resistance in breast cancer. Anal Bioanal Chem. 2016;408(26):7491–503.
22. Teng Y, Girvan AC, Casson LK, et al. AS1411 alters the localization of a complex containing protein arginine methyltransferase 5 and nucleolin. Cancer Res. 2007;67(21):10491–500.
23. Jain N, Zhu H, Khashab T, et al. Targeting nucleolin for better survival in diffuse large B-cell lymphoma. Leukemia. 2018;32(3):663–74.
24. Fletcher JI, Williams RT, Henderson MJ, Norris MD, Haber M. ABC transporters as mediators of drug resistance and contributors to cancer cell biology. Drug Resist Updat. 2016;26:1–9.
25. Lu SX, Abdel-Wahab O. Genetic drivers of vulnerability and resistance in relapsed acute lymphoblastic leukemia. Proc Natl Acad Sci U S A. 2016;113(40):11071–3.
26. Valentin R, Grabow S, Davids MS. The rise of apoptosis: targeting apoptosis in hematologic malignancies. Blood. 2018;132(12):1248–64.
27. Shafat MS, Gnaneswaran B, Bowles KM, Rushworth SA. The bone marrow microenvironment - Home of the leukemic blasts. Blood Rev. 2017;31(5):277–86.
28. Rahgozar S, Moafi A, Abedi M, et al. mRNA expression profile of multidrug-resistant genes in acute lymphoblastic leukemia of children, a prognostic value for ABCA3 and ABCA2. Cancer Biol Ther. 2014;15(1):35–41.
29. Fernandes E, Freitas R, Ferreira D, et al. Nucleolin-Sle A Glycoforms as E-Selectin Ligands and Potentially Targetable Biomarkers at the Cell Surface of Gastric Cancer Cells. Cancers (Basel). 2020;12(4).
30. Gilles ME, Maione F, Cossutta M, et al. Nucleolin Targeting Impairs the Progression of Pancreatic Cancer and Promotes the Normalization of Tumor Vasculature. Cancer Res. 2016;76(24):7181–93.
31. Modena P, Buttarelli FR, Miceli R, et al. Predictors of outcome in an AIEOP series of childhood ependymomas: a multifactorial analysis. Neuro Oncol. 2012;14(11):1346–56.
32. Marcel V, Catez F, Berger CM, et al. Expression Profiling of Ribosome Biogenesis Factors Reveals Nucleolin as a Novel Potential Marker to Predict Outcome in AML Patients. PLoS One. 2017;12(1):e0170160.

33. Chen Z, Shi T, Zhang L, et al. Mammalian drug efflux transporters of the ATP binding cassette (ABC) family in multidrug resistance: A review of the past decade. Cancer Lett. 2016;370(1):153–64.
34. Maik-Rachline G, Seger R. The ERK cascade inhibitors: Towards overcoming resistance. Drug Resist Updat. 2016;25:1–12.
35. Inder KL, Lau C, Loo D, et al. Nucleophosmin and nucleolin regulate K-Ras plasma membrane interactions and MAPK signal transduction. J Biol Chem. 2009;284(41):28410–9.
36. Tomiyasu H, Watanabe M, Sugita K, et al. Regulations of ABCB1 and ABCG2 expression through MAPK pathways in acute lymphoblastic leukemia cell lines. Anticancer Res. 2013;33(12):5317–23.
37. Farin K, Schokoroy S, Haklai R, et al. Oncogenic synergism between ErbB1, nucleolin, and mutant Ras. Cancer Res. 2011;71(6):2140–51.
38. Liao ZX, Chuang EY, Lin CC, et al. An AS1411 aptamer-conjugated liposomal system containing a bubble-generating agent for tumor-specific chemotherapy that overcomes multidrug resistance. J Control Release. 2015.

Figures

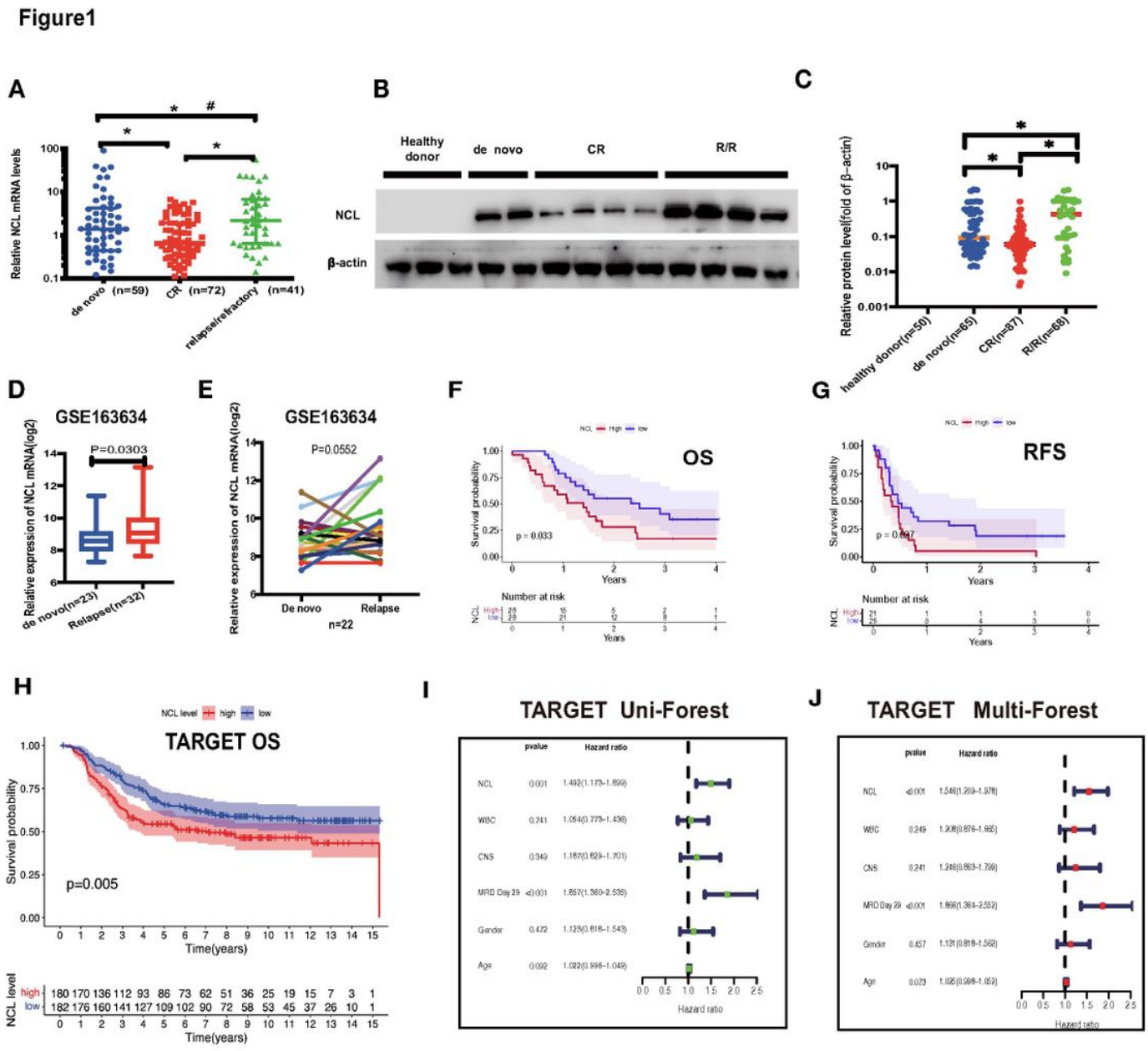

Figure 1

NCL is overexpressed in ALL cells and significantly correlated to poor survival. (A) Figure1. NCL is overexpressed in ALL cells and significantly correlated to poor survival. (A) Expression level of NCL mRNA was determined by qRT-PCR. Compared with healthy donors. (B-C) NCL protein expression in samples of healthy donors, and ALL patients with de novo, CR status and refractory/relapse status was detected by western blot (B). The quantification of expression of NCL protein was highest in the refractory/relapse, followed by the de novo and CR status. The healthy donors showed no expression of NCL(C).(D-E) Relative expression level of NCL mRNA data of GSE163634 gene expression profile from GEO database. (D)Relative expression data of NCL mRNA in the de novo group(n=23) and relapse group(n=32). (E) Relative expression level of NCL mRNA in the longitudinal specimens collected from patients at diagnosis

and relapse. (F, G) Prognostic analysis of high-level of NCL mRNA and low-level of NCL mRNA in de novo ALL patients.Kaplan-Meier survival curve analysis of OS(F) and RFS (G) in the high-level (read line) and low-level (blue line) patients in our patient set(P=0.033, P=0.027 respectively). (H-J) Prognostic analysis of high-level of NCL mRNA and low-level of NCL mRNA in ALL patients of an additional data set downloaded from TARGET database. (H) Kaplan-Meier survival curve analysis of OS in the high-level (read line) and low-level (blue line) patients in additional data set (P=0.005). (I-J) Prognostic prediction value of NCL and other variable prognostic risk models in additional Set. (I) Univariate Cox regression analysis of OS. (J) Multivariate Cox regression analysis of OS. CNS, Central Nervous System. MRD D29: minimal residual disease at day 29 after initial treatment. #: overall comparison, P>0.05. *: pairwise comparison, P<0.05.

Figure 2

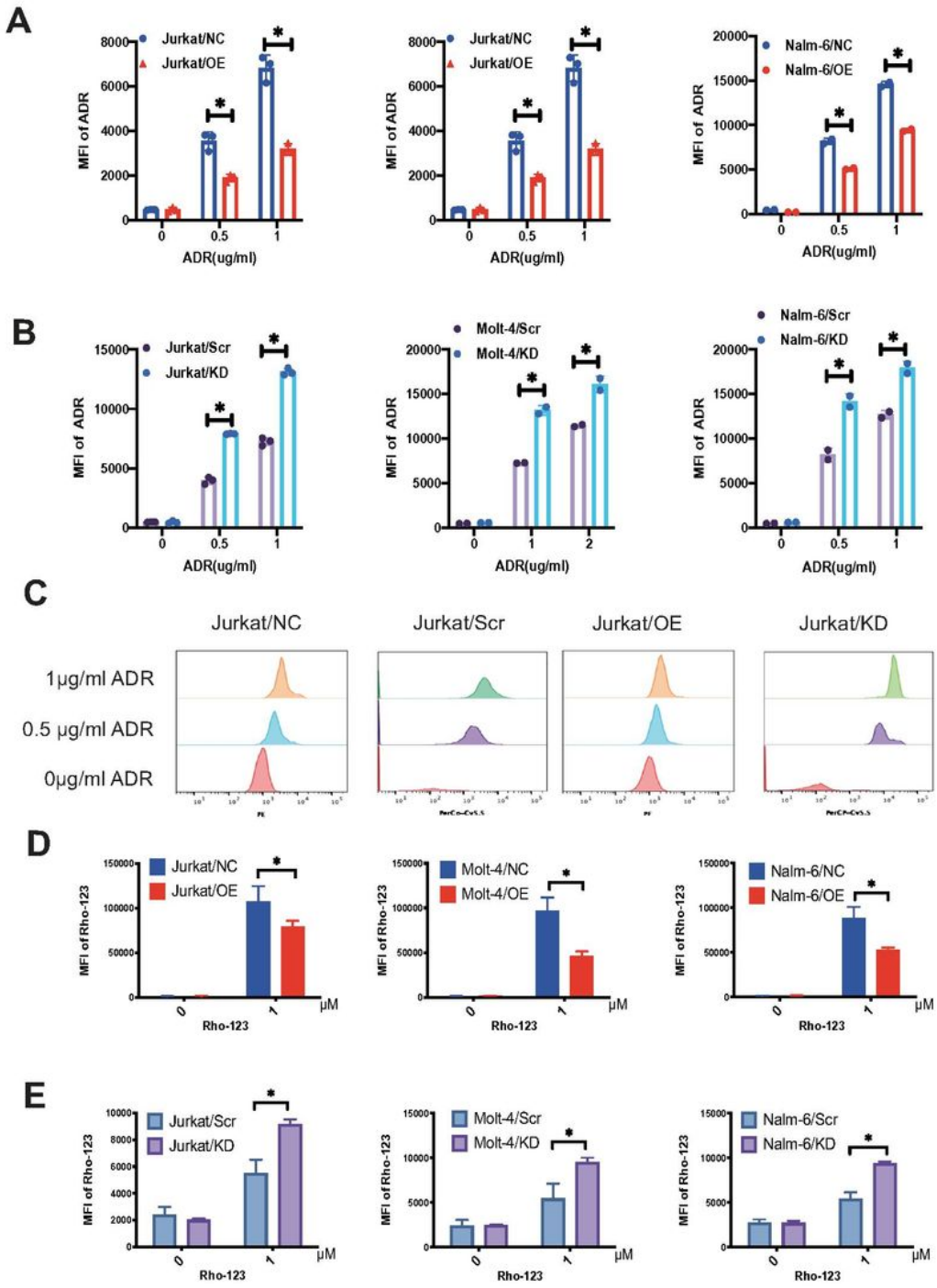

Figure 2

Nucleolin (NCL) facilitates drug efflux from acute lymphoblastic leukemia (ALL) cells. (A, B) Intracellular adriamycin (ADR) accumulation assay was measured by flow cytometry after exposure in different ADR concentrations, the intracellular ADR MFI in OE, NC, KD, and Scr lines of Jurkat, Molt-4 and Nalm-6 cells were analyzed. (C) The respensitive flow cytometry histograms of the changes with different concentrations intracellular ADR in Jurkat NC, Scr, OE and KD lines. (D, E) The effect of NCL on cellular

drug efflux was also confirmed by Rho123 efflux test. The intracellular Rho-123 MFI in OE, NC, KD, and Scr lines of Jurkat, Molt-4 and Nalm-6 cells were analyzed. The results are in accordance with IC50 test and intracellular ADR accumulation assay. *, P < 0.05.

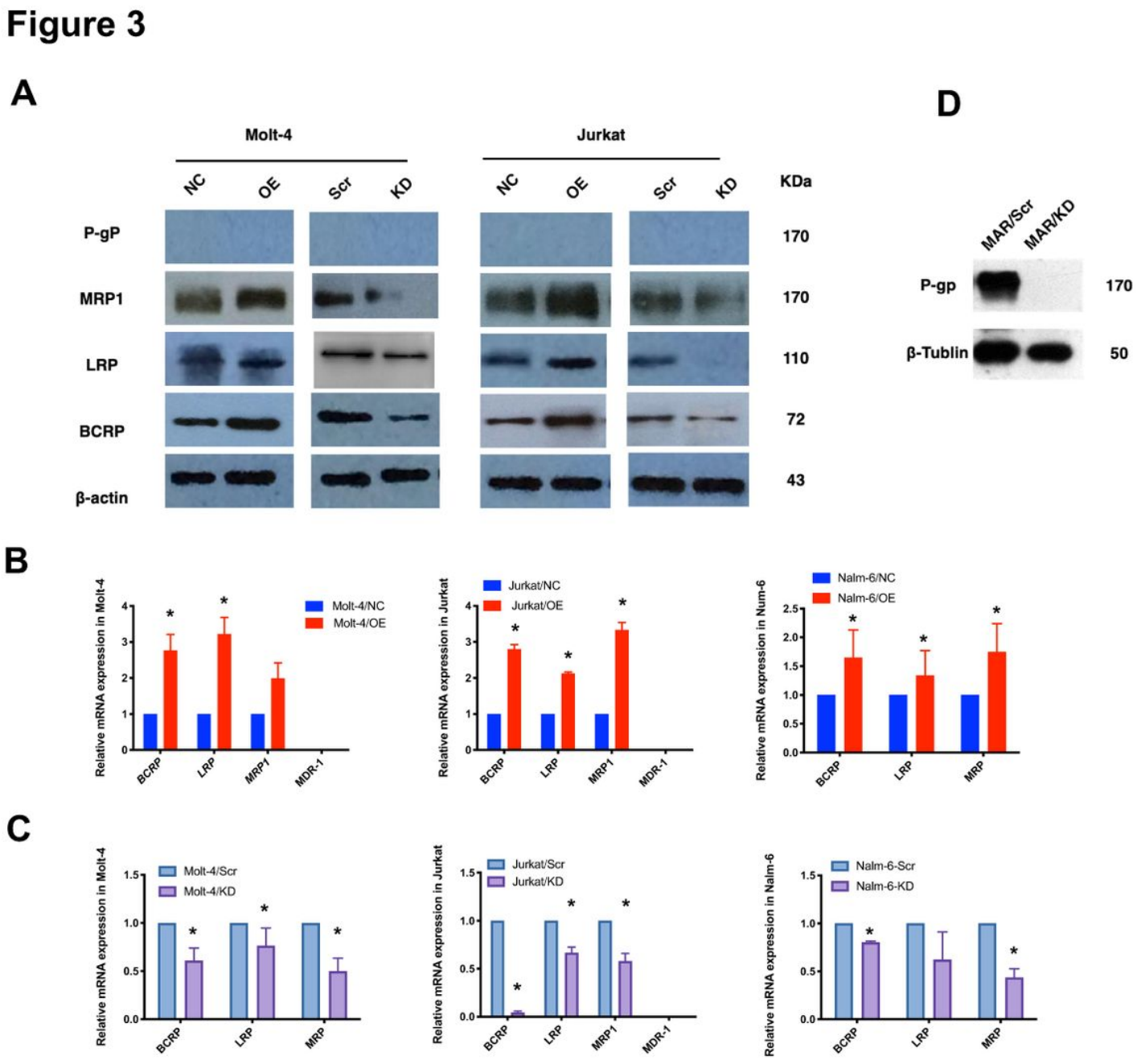

Figure 3

Nucleolin (NCL) regulates the expression of ABC (ATP-binding cassette) transporters. (A) Western blot analysis was used to detect the BCRP, MRP1, LRP, and MDR1 expression at the protein level in Jurkat and Molt-4 cells. β-actin was utilized to monitor an equal loading of proteins. (B, C) qRT-PCR experiments were performed to examine the expression of BCRP, MRP1, LRP, and MDR1 mRNA; results are in accordance

with western blot. * P < 0.05. (D) Compared to MAR transfected counterparts, MDR1 (p-gp) protein was expressed in MAR/Scr, but not in MAR/KD. β-Tublin was utilized to monitor an equal loading of proteins.

Figure4

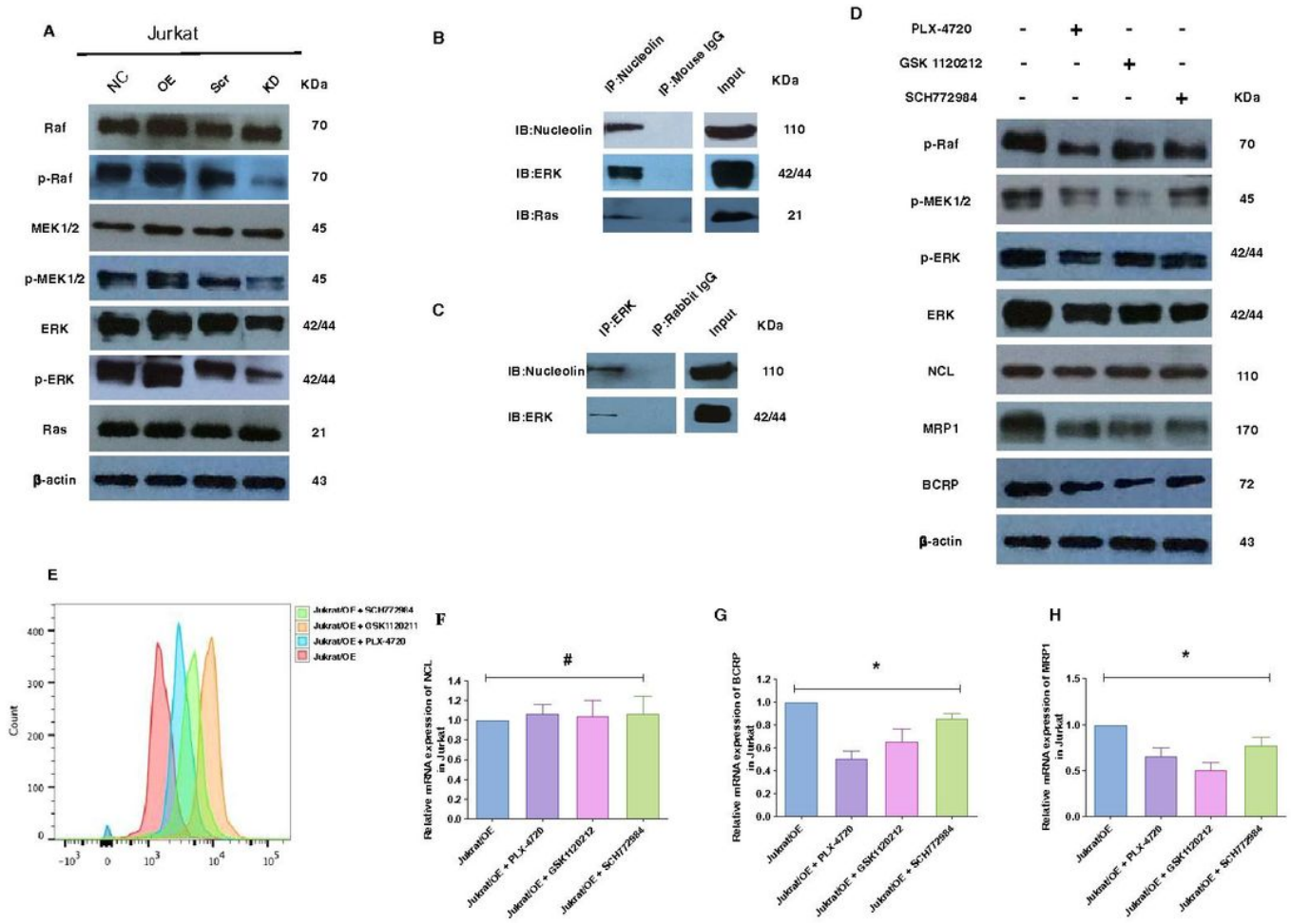

Figure 4

Role of the ERK pathway in the modulation of drug resistance by nucleolin (NCL). (A) Western blot analysis of the protein and the corresponding phosphorylated protein levels of the ERK pathway (Ras/Rf/MEk1/2/ERK) in response to overexpressed or silenced NCL ex- pression in Jurkat/NC, OE, Scr and KD cells. (B, C) NCL-ERK interaction and NCL-Ras interaction were confirmed by co-IP tests in whole-cell lysates of Jurkat cells. (D) The effect of inhibiting ERK signaling activity on drug resistance was examined by western blot in Jurkat/OE cells. (E) Effect of inhibiting ERK signaling activity on drug resistance was determined using intracelluar ADR accumulation analysis by flow cytometry in Jurkat/OE cells. (F-G) qRT-PCR was used to detect the mRNA levels of NCL, BCRP, and MRP1 after ERK pathway inhibition in Jurkat/OE cells. * P < 0.05. # P > 0.05.

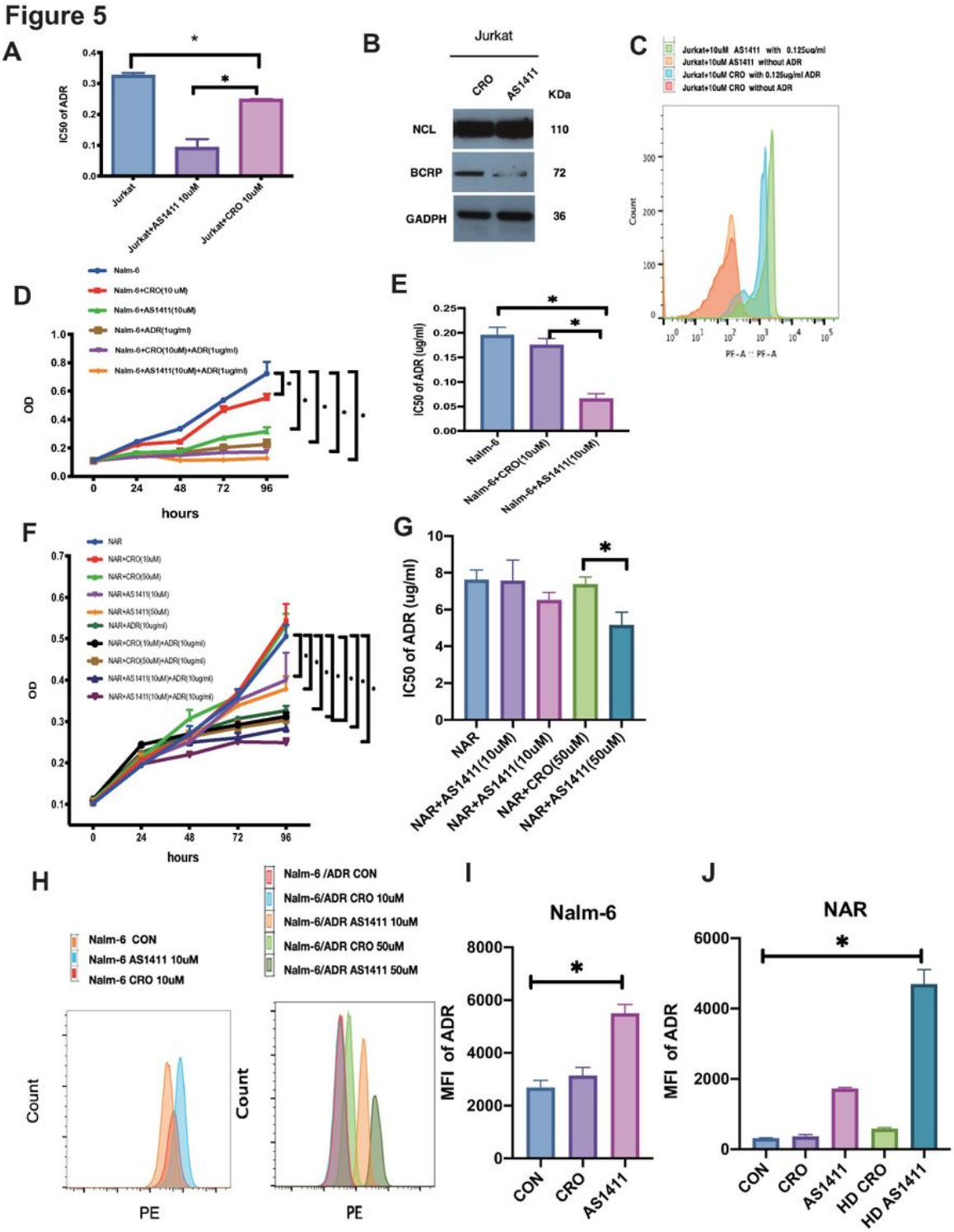

Figure 5

Targeting nucleolin (NCL) by AS1411 increased drug sensitivity and reverses resistance in acute lymphoblastic leukemia (ALL) cells. (A) Decreased drug resistance of adriamycin (ADR) was observed in AS1411-treated Jurkat cells using MTT test. **(B)** AS1411 decreased the expression of BCRP protein expression, without affecting NCL expression using a western blot assay. **(C)** By FCM, more intracellular ADR MFI were detected in AS1411 treated ALL primary cells. **(D, F)** Effects on cell growth of AS1411 were

examined by MTT assay on Nalm-6 cells and Nalm-6/ADR lines. (**E, G**) Effect of inhibiting NCL using AS1411 on cellular ADR sensitivity was evaluated by IC50 analysis. (**H, I, J**) Intracellular drug accumulation assay was measured by flow cytometry. After exposure in AS1411 or CRO with or without ADR for 12 h, the percentage of ADR accumulation cells and MFI were calculated by flow cytometry. * $P <$ 0.05.

Figure6

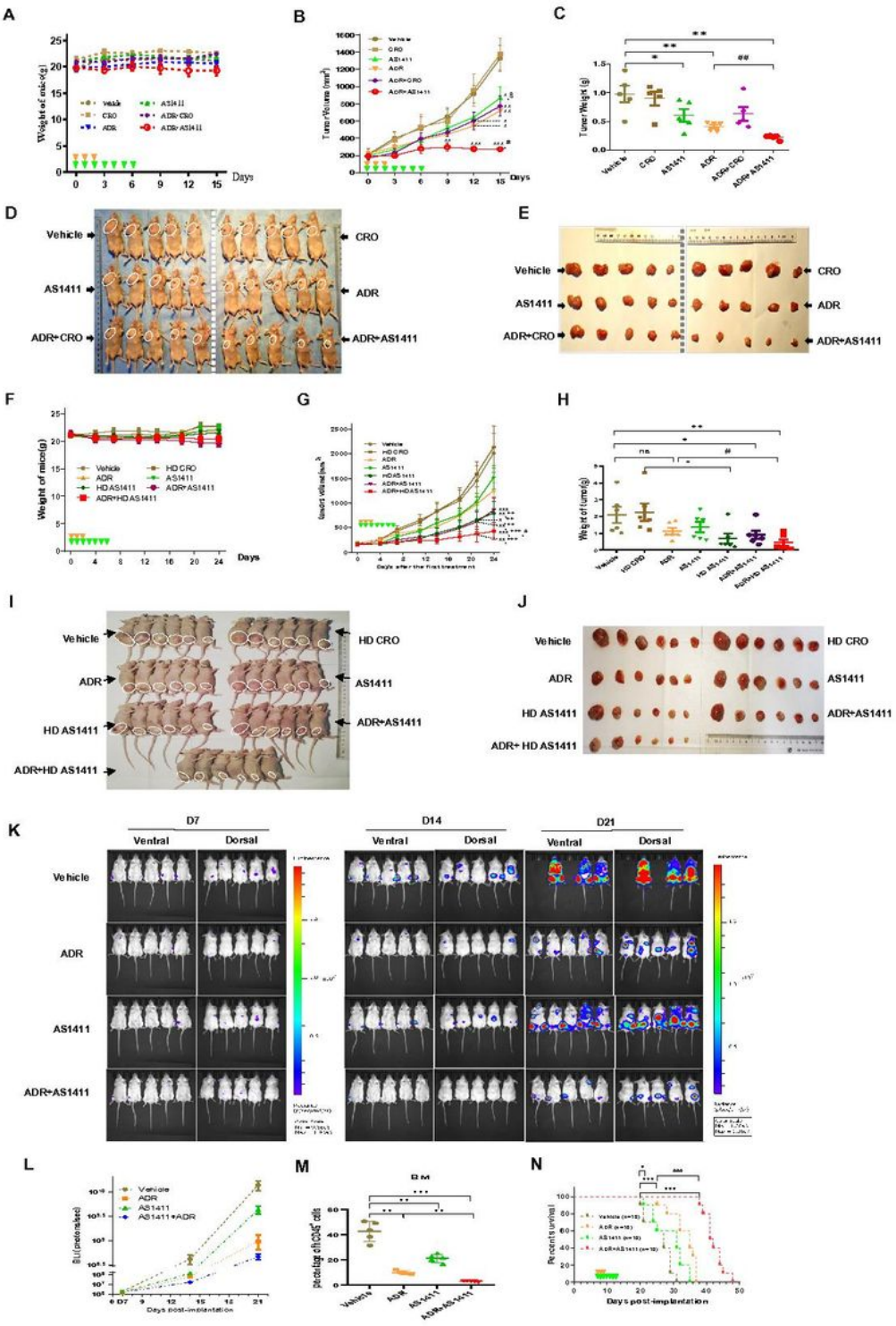

Figure 6

Targeted inhibition of NCL by AS1411 sensitized ADR treatment ALL cell-derived xenograft mouse models. (A-D) No significant reduction of Nalm-6-derived mice body weight was observed during the treatments(A). At 3 weeks after injection, 30 Nalm-6 nude mice with comparable tumor size (200±80mm^3) were randomly divided into 6 groups with different treatments. Tumor volumes were calculated at the indicated days (B). * P< 0.05; ** P< 0.01; *** P < 0.001 versus vehicle on same day; ++ P < 0.01 versus CRO on the same day; # P < 0.05 versus ADM on the same day. 15 days after the first treatment, tumor tissues from all mice were photographed (D, E) and weighted (C). * P< 0.05; ** P< 0.01versus vehicle; ## P < 0.01 versus ADM. (F-J) No significant reduction of Nalm-6/ADR-derived mice body weight was observed during the treatments(F). Similarly, at 18 days after injection, 42 Nalm-6/ADR nude mice with comparable tumor size (165.9±64.3 mm^3) were randomly divided into 7 groups with different treatments. The tumor volumes were calculated at the indicated days and graphed (G). * P< 0.05; ** P< 0.01; *** P < 0.001 versus vehicle on same day; ++ P < 0.01; +++ P < 0.001 versus HD CRO on the same day; # P < 0.05 versus ADR on the same day. 24 days after the first treatment, tumor tissues from all the sacrificially mice were photographed (I, J) and weighted (H). ns P≥0.05; * P< 0.05; ** P< 0.01 versus vehicle; +P < 0.05 versus CRO; # P < 0.05versus ADM. (K-N), One week later after injection, Luc+Nalm-6 NCG mice received different treatments. Twice a week (at the 4th and 7th day), the bioluminescence intensity of the injected mice was assessed (K), and representative images were shown as (L), at 7,14 and 21 days after Luc+Nalm-6 cells injection (n=3 or 5). Two mice died of progression disease before the detection of bioluminescence intensity at day 21. 2 weeks after the first dose of treatment, mice in each group were sacrificed, and leukemia burden (human CD45+ cells) in one marrow was determined by flow cytometry (M) (n=3 or 5). ** P< 0.01; *** P < 0.001 versus vehicle; ## P < 0.01 versus ADM. Following the same experimental procedure, the survival rate and survival time of NCG mice in each treatment group were evaluated, the survival of mice is shown as Kaplan-Meier curves (n=10) N).* P< 0.05; *** P < 0.001 versus vehicle; ### P < 0.001 versus ADR.

Figure 7

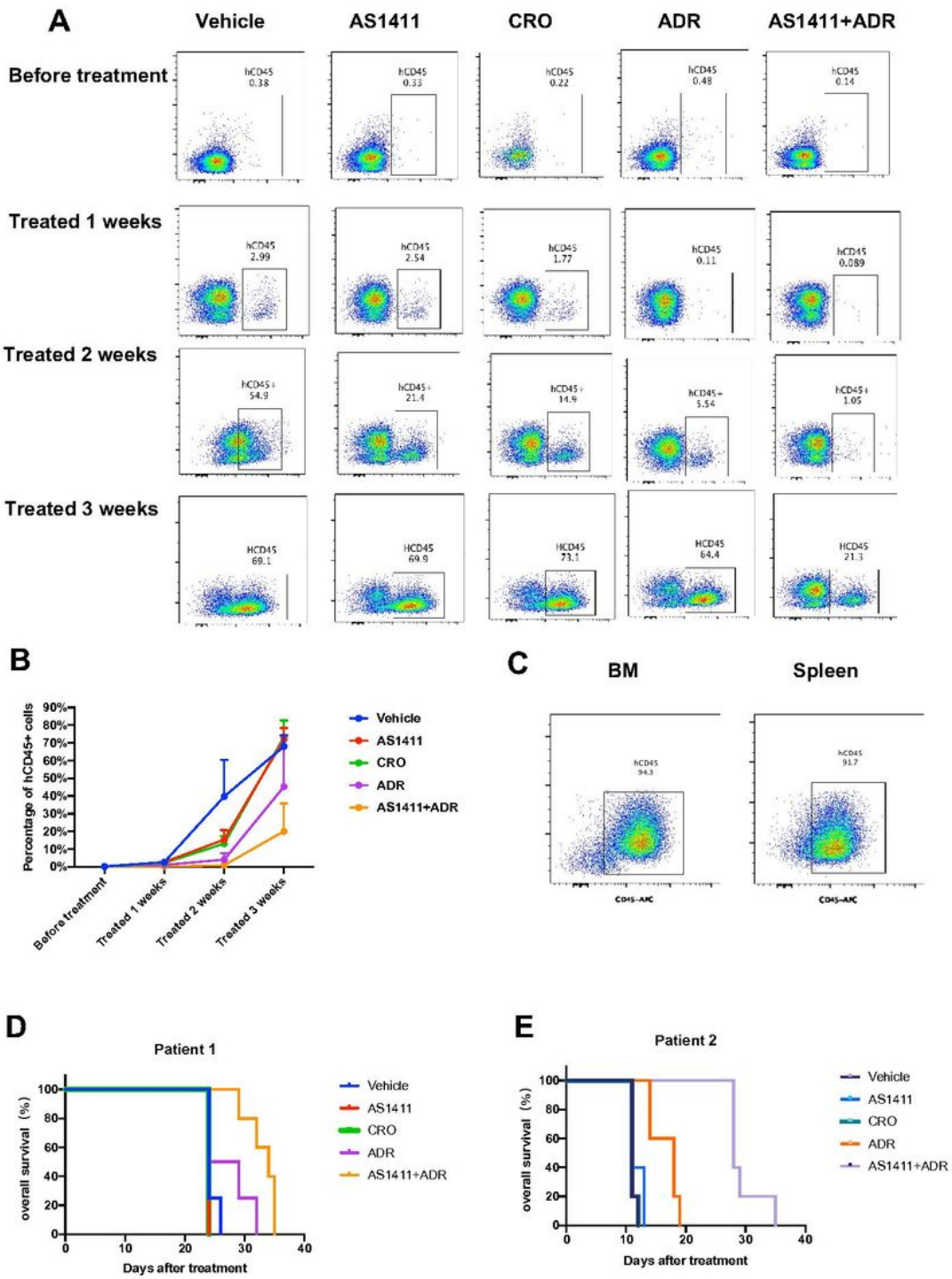

Figure 7

Targeted inhibition of NCL by AS1411 sensitized ADR treatment patient-derived xenograft mouse models. **(A)** Detection of hCD45+ cells in the peripheral blood of the leukemic mice in the patient 1 at time point of before treatment, treated 1 weeks, treated 2 weeks, and treated 3 weeks using FACS. **(B)** The curve of numbers of hCD45+ cells in the different time point in the different treatment groups. **(C)** Detection of

hCD45+ cells in the bone marrow and spleen in the mice with morbidity. Survival of patients 1-derive mice **(D)** and patients 2-derive mice **(E)** is shown as Kaplan-Meier curves.

Supplementary Files

This is a list of supplementary files associated with this preprint. Click to download.

- Supplementaryfile.docx